Received: 19 August 2025 | Accepted: 27 October 2025

DOI: 10.1111/ics.70052

International Journal of Cosmetic Science
SOCIÉTÉ FRANÇAISE DE COSMÉTOLOGIE

ORIGINAL ARTICLE

# Scale-robust fibre orientation analysis of hair using two-dimensional Fourier transform

**Motoki Takeda**[1,2] | **Sinyoung Lee**[1] | **Ken Kiyono**[1]

[1]Graduate School of Engineering Science, The University of Osaka, Toyonaka, Osaka, Japan

[2]Development Headquarters, Milbon Co., Ltd., Osaka, Osaka, Japan

**Correspondence**
Motoki Takeda, Graduate School of Engineering Science, The University of Osaka, 1-3 Machikaneyama-cho, Toyonaka, Osaka 560-8531, Japan.
Email: mtakeda@bpe.es.osaka-u.ac.jp

## Abstract

**Objective:** To address the current lack of standardized tools for evaluating hair appearance in the beauty industry, this study presents a robust and accessible method for objectively quantifying hair fibre orientation using two-dimensional discrete Fourier transform (2D-DFT).

**Methods:** We analysed hair images of 120 Japanese women using 2D-DFT and extracted the principal orientation angle and anisotropy index by fitting an ellipse to the directional Fourier spectrum. The robustness of the method at the image scale was tested by evaluating its performance across various image resolutions.

**Results:** The proposed method accurately quantified hair orientation and showed consistent performance across differing image scales provided that individual hair fibres were visually distinguishable. As the method requires only standard digital images and basic computational processing, it is well suited for practical applications.

**Conclusion:** Our 2D-DFT-based approach offers a simple yet robust framework for analysing overall hair orientation. Although further validation is required for different hair types and local orientation analyses, this method provides a foundation for objective evaluation of hair appearance in cosmetic diagnostics and hair science research.

KEYWORDS

computer modelling, Fourier transform, hair fibre orientation, hair treatment, image analysis, statistics

## Résumé

**Objectif:** Afin de pallier l'absence d'outils standardisés pour évaluer l'apparence des cheveux dans l'industrie cosmétique, cette étude propose une méthode robuste et accessible permettant de quantifier objectivement l'orientation des fibres capillaires à l'aide de la transformée de Fourier discrète bidimensionnelle (2D-DFT).

**Méthodes:** Des images capillaires de 120 femmes japonaises ont été analysées par 2D-DFT. L'angle d'orientation principal et l'indice d'anisotropie ont été

extraits en ajustant une ellipse au spectre directionnel de Fourier. La robustesse de la méthode a été évaluée en fonction de la résolution des images.

**Résultats:** La méthode proposée permet une quantification précise de l'orientation capillaire et montre une performance constante à travers différentes échelles d'image, à condition que les fibres capillaires soient visuellement discernables. Étant donné qu'elle ne nécessite que des images numériques standards et un traitement informatique de base, cette approche est bien adaptée aux applications pratiques.

**Conclusion:** Notre approche basée sur la 2D-DFT offre un cadre simple mais robuste pour l'analyse de l'orientation globale des cheveux. Bien qu'une validation supplémentaire soit nécessaire pour différents types de cheveux et pour des analyses locales, cette méthode constitue une base solide pour une évaluation objective de l'apparence capillaire dans les diagnostics cosmétiques et la recherche en science capillaire.

## INTRODUCTION

Scalp hair not only serves biological functions, such as protecting the head from heat, cold and physical impacts, but also plays important social and psychological roles [1]. Culturally, hair appearance historically reflects sex, age, occupation and personal values [2]. Psychologically, this relationship is closely related to self-expression and perceived attractiveness [3]. Acknowledging these roles, people have long paid close attention to their hair, engaging in various beauty practices and treatments to maintain or modify their appearance. These practices include haircuts to adjust length and texture, blow-drying and hot ironing to alter volume and curl and colouring or perming to change colour and shape.

Despite their widespread use, these beauty treatments often result in adverse effects, including hair breakage, frizz and hair loss [4–6]. Hair appearance changes naturally with age, resulting in greying, thinning and loss of hair [7, 8]. These undesirable changes are a common source of frustration and have driven significant efforts in the beauty industry to develop products and treatments to address these concerns.

Hair orientation is a key factor that influences the overall appearance and aesthetic perception of hair. Hair orientation is determined by two main aspects: the morphological structure of individual hair fibres and the alignment of multiple fibres. The first aspect, the morphological structure, determines whether a single hair fibre is straight, wavy, curly or coily. Quantitative evaluation methods, such as those used to assess curliness and waviness, have effectively captured the global diversity of hair fibre morphology, offering valuable insights into hair characteristics across different populations [9, 10].

Hair fibre alignment refers to whether neighbouring fibres are uniformly orientated in the same direction. Because the visual appearance of hair is determined by the collective behaviour of approximately 100 000 individual strands [11], fibre alignment plays a critical role in shaping hair perception. Despite the significance of this aspect, quantitative methods for analysing hair alignment remain poorly developed. This limitation presents a major challenge as it hinders the comprehensive evaluation of hair appearance. Addressing this gap is essential for advancing our understanding of hair aesthetics and developing reliable techniques to assess and improve fibre alignment.

Image-based measurement and analysis techniques offer promising approaches for characterizing hair appearance. To date, three representative methods have been proposed for the quantitative evaluation of hair orientation.

The first involves image acquisition using a near-infrared polarized light source, which enables visualization and quantification of hair fibre orientation by exploiting the anisotropic properties of the internal hair structure [12]. This method provides a highly precise evaluation of individual fibre orientations and is robust against variations in hair colour. However, its application is limited owing to the requirement for specialized equipment.

Second, the histogram of oriented gradients (HOG) method, which calculates image gradients, has been applied to analyse the orientation of hair bundles [13, 14]. This approach quantifies the effects of hair care products on bundle alignment. However, it has notable limitations. Most angular information is lost because of the quantization of orientations into only eight bins during histogram construction.

McMullen et al. applied a two-dimensional discrete Fourier transform (2D-DFT) to analyse hair fibre orientation [15]. This technique is widely used to assess the orientation of fibrous materials [16–18]. In their study, 2D-DFT was employed to quantitatively evaluate the straightening effects of relaxer treatments on African hair, which is characterized by a tightly coiled morphology. However, the applicability of this method to other hair types, particularly those with different morphological structures or colours, has not been examined. Consequently, the broader potential for analysing hair orientation remains largely unexplored.

Despite the various methods proposed to date, there is a lack of a standardized approach for hair orientation analysis. Previous studies identified three essential criteria for establishing a widely accessible method: accuracy, robustness and simplicity. In image analysis, major advances have often been driven by techniques that are robust to environmental factors, such as image scale, rotation, noise and variations in lighting conditions [13, 19]. Among these criteria, simplicity is particularly important for ensuring broad usability and accessibility. Diagnostic systems for evaluating hair conditions based on hair orientation analysis are increasingly being sought as practical tools in the beauty industry. For widespread adoption, such systems must be user-friendly and require minimal technical expertise and no specialized knowledge. However, the development of a method that combines robustness and ease of use remains challenging.

In this study, we propose a hair orientation analysis method based on the 2D-DFT. The method was designed to operate with simple equipment while maintaining robustness at the image scale, making it suitable for practical applications. The following sections describe the data set used, outline the procedure for analysing hair images and assess the scale robustness of the proposed approach. We then present the results obtained by applying this method to hair images and demonstrate its consistency and reliability. Finally, we discuss the implications of our findings, acknowledge the limitations of the method and suggest directions for future research.

# DATA AND METHODS

## Hair image data

Our data set consisted of 120 samples collected from Japanese females aged 20–69 years, with a mean age of 42.1 years and a standard deviation of 12.2 years. To evaluate hair in its natural state, participants were instructed to avoid using hair cosmetics or undergoing cosmetic treatment on the day of the study.

All participants were informed of the purpose and methodology of the study, and written informed consent was obtained before data collection. Ethical approval was granted by the Brain Care Clinic Institutional Review Board (IRB) under protocol number 20171211 and management number BCC241003-5.

Photographs of the back of each participant's head were captured using a NIKON D5300 camera under controlled lighting on a consistent scale. The original images had a resolution of 2000 × 2992 pixels and a depth of 24 bits. The pixel size was approximately 0.1 mm/pixel, which is slightly larger than the diameter of individual hair fibres (0.06–0.1 mm) [8, 20]. To isolate the hair region, images were cropped to 512 × 512 pixels. Figure 1 shows representative examples of the cropped hair images included in the data set.

The data set captured variations in coloration and morphology. The colour ranges from black to pale yellow, including natural grey and artificially dyed hair, with colours often varying along individual strands and across different areas of the scalp. Morphologically, the fibres range from straight to wavy and exhibit diverse orientation patterns and crimp structures. Although the data set was limited to Japanese females, it included substantial intra- and inter-individual variations, providing a robust foundation for subsequent analysis.

## Image pre-processing

Most hair images in the data set exhibited straight or wavy textures with colours ranging from black to yellow. These images were converted to grayscale using the OpenCV algorithm: $Y = 0.299\,R + 0.587\,G + 0.114\,B$, where $R$, $G$ and $B$ represent the red, green and blue channels, respectively, and $Y$ denotes the grayscale value [21]. To prepare for the orientation analysis, the mean intensity of each grayscale image was normalized to zero.

## Fundamental principles of fibre orientation analysis

First, we describe the fundamental principles of fibre orientation analysis using the 2D-DFT, as illustrated in Figure 2. The 2D-DFT is a mathematical operation that transforms an image from the spatial domain to the frequency domain, known as the Fourier spectrum. It represents an image as a linear combination of sinusoidal plane waves, each defined by a specific spatial frequency, orientation angle and amplitude. As shown in Figure 2a,b, if an image contains only a single sinusoidal plane wave, the 2D-DFT produces two point-symmetric peaks in the frequency domain. The radial distance of these peaks from

**FIGURE 1** Representative examples of 512×512 pixel-cropped hair images collected from participants, illustrating the diversity of colour and texture present in the data set.

the origin corresponded to the frequency, their angular positions indicated the orientation, and the peak intensities reflected the contribution of the waves to the image.

In real-world images, a spectrum comprises multiple wave components, resulting in a distributed spectral pattern. When the fibres are nearly parallel (Figure 2c), their spectral distribution is concentrated within a narrow angular sector, indicating that the images comprise waves with similar orientations. By contrast, a broader angular distribution in the spectrum suggests more varied fibre directions (Figure 2d). By quantifying this angular dispersion, for example, using the ratio of the total amplitude of the Fourier spectrum across the angles, we can obtain a quantitative measure of the orientation distribution. This enables the extraction of both the principal orientation angle and its variability, offering a comprehensive analysis of hair fibre orientation.

## Procedure of hair fibre orientation analysis

A digital image of size $N \times N$ pixels is represented as a 2D matrix of pixel values $z(x,y)$, where $N$ denotes an even number, and $x,y$ are spatial coordinates. The 2D-DFT of $z(x,y)$ is defined as

$$F(k,l) = \sum_{x=0}^{N-1}\sum_{y=0}^{N-1} z(x,y)\exp\left\{-2\pi i\left(\frac{k}{N}x + \frac{l}{N}y\right)\right\}, \quad (1)$$

where $i = \sqrt{-1}$, and $k,l \in \{0,1,\cdots,N-1\}$ represent the frequency indices mapped to spatial frequency domain along the $x$ and $y$ axes, respectively. These spatial frequencies are defined as

$$f_x = -\frac{1}{2} + \frac{k}{N}, f_y = -\frac{1}{2} + \frac{l}{N}. \quad (2)$$

The Fourier spectrum $S_{\text{ortho}}(k,l)$ is then calculated as the magnitude of the $F(k,l)$ raised to the power of $q$:

$$S_{\text{ortho}}(k,l) = |F(k,l)|^q. \quad (3)$$

This spectrum is converted into polar coordinates, $S_{\text{polar}}(r,n)$, where $r = \sqrt{k^2+l^2}$ denotes the index of radial frequency and $n = \tan^{-1}\left(\frac{l}{k}\right)$ represents the orientation angle. The spectrum is then resampled onto a uniform polar grid, as follows:

$$\{(f_r,\theta_n)\} = \left\{\left(\frac{r}{N}, \frac{2\pi n}{360}\right)\right\}, \quad (4)$$

where $r$ and $n$ represent integers satisfying $0 \le r < N/2$ and $0 \le n < 360$, respectively. Resampling was performed by bilinear interpolation, and the resampled radial spectrum $S_{\text{polar}}(f_r,\theta_n)$ was obtained [18].

The orientation distribution $P(\theta)$ is then calculated by summing the resampled spectrum $S_{\text{polar}}(f_r,\theta_n)$ for each directional angle over all radial frequencies satisfying $f_{\min} \le f_r$, and then normalizing such that $P(\theta) = 1$. This is expressed as follows:

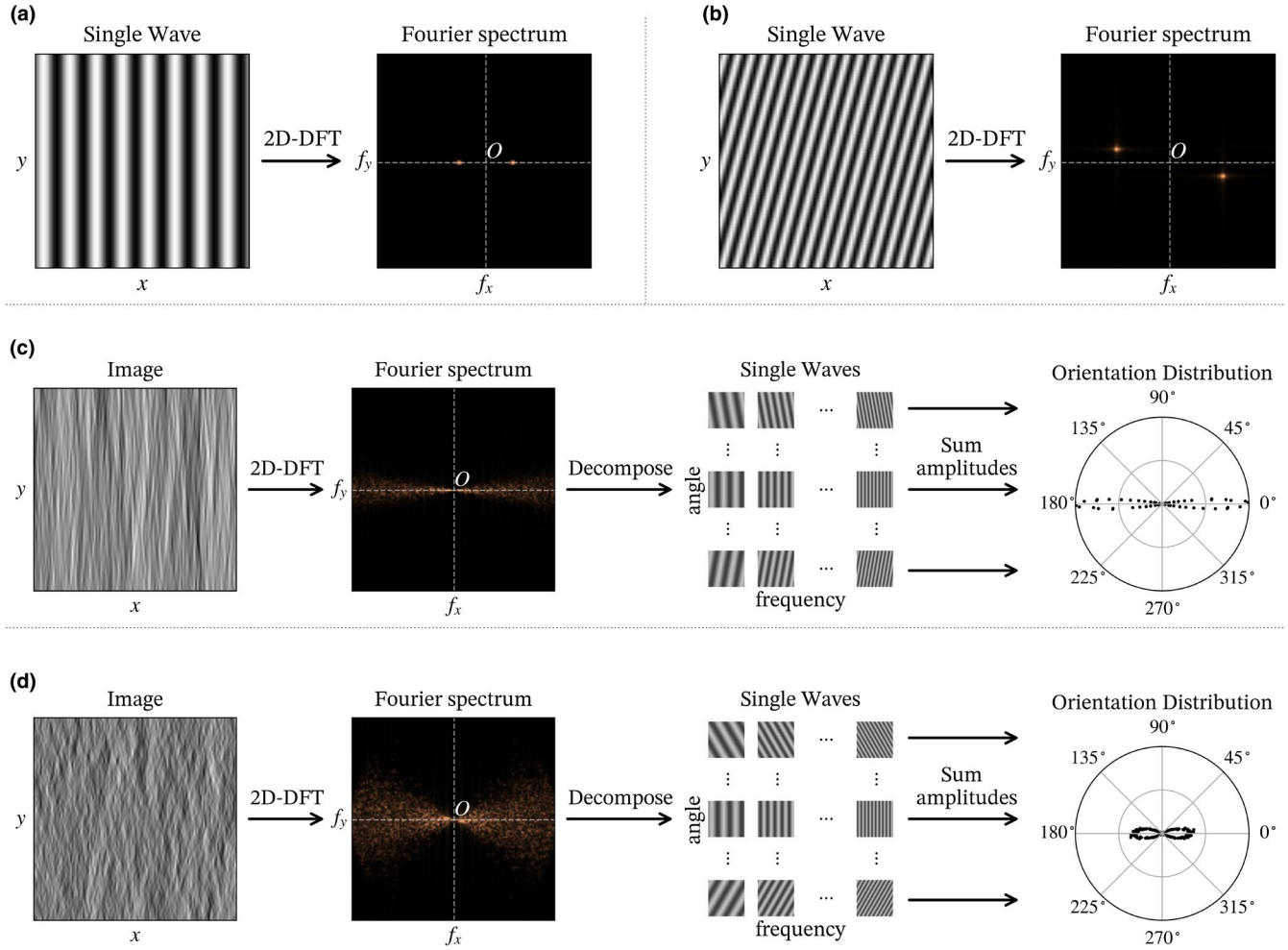


**FIGURE 2** Schematic illustration of fibre orientation analysis based on the two-dimensional discrete Fourier transform (2D-DFT). The top row shows how sinusoidal plane waves are transformed into their corresponding Fourier spectra in the spatial frequency domain $(f_x, f_y)$: (a) Low-frequency wave aligned along the *x*-axis and (b) higher frequency wave oriented diagonally. The subsequent rows depict the orientation analysis workflow. (c) From left to right: An image of highly aligned fibres; its corresponding Fourier spectrum; spectral decomposition into constituent sinusoidal components; and the resulting sharp orientation distribution, where radial distance indicates the summed amplitude for each orientation angle. (d) Contrasting image with less aligned fibres yielding a more diffuse spectrum and a broader orientation distribution.

$$P(\theta) = \frac{\sum_{r=\lceil Nf_{\min} \rceil}^{\frac{N}{2}} S_{\text{polar}}(f_r, \theta_n)}{\sum_{n=0}^{359} \sum_{r=\lceil Nf_{\min} \rceil}^{\frac{N}{2}} S_{\text{polar}}(f_r, \theta_n)}, \tag{5}$$

where $\lceil \cdot \rceil$ denotes the ceiling function. In particular, $\lceil Nf_{\min} \rceil$ provides the smallest integer index such that the corresponding spatial frequency exceeds $f_{\min}$. The choice of $f_{\min}$ is crucial because it sets the lower bound of the spatial frequencies included in the orientation distribution. A higher $f_{\min}$ not only excludes low-frequency components, such as those caused by nonuniformity in hair colour or large artefacts due to finite-size effects, but may also discard important orientation details. Conversely, a lower $f_{\min}$ retains more details regarding the risk of introducing bias from these low-frequency components.

Feature extraction from the orientation distribution $P(\theta)$ was achieved by fitting an ellipse function $\widetilde{P}(\theta)$ to the distribution, as described in Equation (6). The parameters of the ellipse, including the major and minor axes lengths $a$ and $b$, and the angle $\phi$ between the major axis and the *x*-axis, were estimated by minimizing the least-squares error between $P(\theta)$ and $\widetilde{P}(\theta)$.

$$\widetilde{P}(\theta) = \frac{a^2 b^2}{a^2 \sin^2(\theta + \phi) + b^2 \cos^2(\theta + \phi)} \tag{6}$$

The orientation features of the hair fibres were then defined as the principal orientation angle $\phi$ and the

anisotropy index $\lambda = 1 - b/a$. The anisotropy index $\lambda$ ranges from $0 \leq \lambda < 1$, where values closer to 1 indicate greater anisotropy and values closer to 0 indicate greater isotropy. The closeness of fit of the elliptical approximation to the orientation distribution was evaluated using the coefficient of determination $R^2$.

Hair fibre orientation analysis was applied to the preprocessed images. To evaluate the natural 2D-DFT spectrum of the hair images, the parameter $q$ in Equation (3) was set to one, and $f_{\min}$ in Equation (5) was set to 0.08 pixel$^{-1}$, demonstrating the best performance in our scale robustness study described in the next section. The applicability of the proposed method was evaluated by applying it to all images in the data set and calculating the directional features $\phi$, $\lambda$ and $R^2$. Furthermore, the effect of hair fibre orientation on the analysis accuracy was evaluated by calculating the Pearson correlation coefficient for $\lambda$ and $R^2$.

## Scale robustness study

To assess the scale robustness of the proposed method, we conducted a series of experiments to simulate the changes in the image scale by reducing the image resolution. The objective was to evaluate how effectively the method maintained its performance at various resolutions. In computer vision, reducing image resolution is a widely accepted approach to simulate a decrease in image scale [19].

Specifically, the original data set images were downsampled to 1/2, 1/4 and 1/8 of their original resolutions using bilinear interpolation. Considering that the original image resolution is 0.1 mm/pixel, these downsampled images correspond to resolutions of 0.2, 0.4 and 0.8 mm/pixel, respectively, effectively simulating the appearance of objects at smaller scales. The orientation features were then calculated for both original and scaled images. The means and standard deviations of the differences in the orientation features ($\Delta\phi$ and $\Delta\lambda$) were computed to quantify the method's robustness.

# RESULTS AND DISCUSSION

## Examples of the proposed method's application

Typical examples of the results obtained using this procedure are shown in Figure 3. Figure 3a illustrates the case of highly aligned hair. The Fourier spectrum $S_{\text{ortho}}(k, l)$ exhibited a sharp signal perpendicular to the hair direction. Consequently, the summation of the resampled spectrum $S_{\text{polar}}(f_r, \theta_n)$ across directions produced a distinct ellipse-like shape. The elliptical approximation using the least-squares method yielded a principal orientation angle $\phi$, high anisotropy index $\lambda = 0.95$ and the coefficient of determination $R^2 = 0.99$.

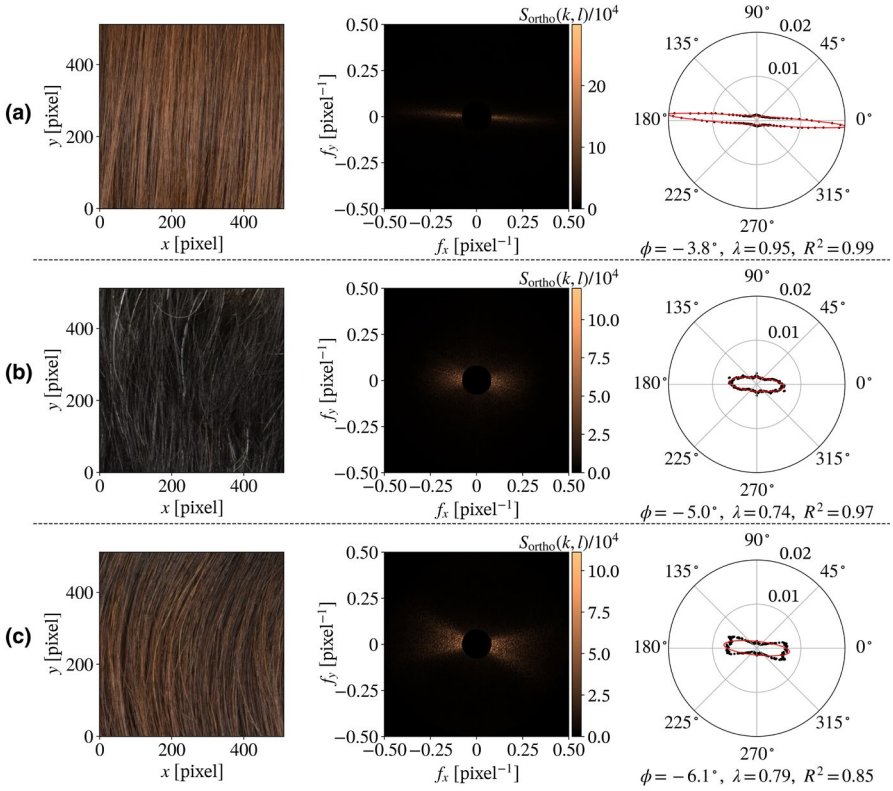


**FIGURE 3** Representative results of fibre orientation analysis for (a) highly aligned, (b) moderately aligned and (c) poorly aligned hair. Each row presents, from left to right: The original hair image, its Fourier spectrum $S_{\text{ortho}}(k, l)$, and the orientation distribution $P(\theta)$ (black dots) overlaid with the fitted elliptical model $\widetilde{P}(\theta)$ (red line). In the Fourier spectra, black regions indicate low-frequency components excluded from the summation in Equation (5).

Figure 3b shows the results for the less aligned hair. In this case, $S_{ortho}(k, l)$ displayed a more diffuse signal, resulting in a broader ellipse-like orientation distribution, with $\lambda = 0.74$ and $R^2 = 0.97$.

Figure 3c shows the case with the poorest fit to the elliptical model $(R^2 = 0.85)$. This image shows wavy hair in two dominant orientations. Consequently, both the Fourier spectrum and orientation distribution revealed two directional peaks. The elliptical approximation returns a value of $\phi$ that reflects the average of the two directions and a lower anisotropy index $\lambda$. For hair images with multiple prominent orientation components, a more accurate characterization may require fitting multiple ellipses or employing more advanced modelling techniques, which remains a topic for future work.

## Data set-wide evaluation of orientation features

We applied the proposed method to all images in our data set and calculated the orientation features $\phi$, $\lambda$ and $R^2$. As shown in Figure 4, the minimum $R^2$ value of 0.85 suggests that the elliptical approximation fits the orientation distribution well and is a reliable approach for analysing hair fibre orientation, except in a few cases with multiple principal directions, as mentioned above.

In addition, we observed a positive correlation between $R^2$ and $\lambda$ ($\rho = 0.57$, $p < 0.001$), indicating that lower fibre alignment tends to reduce the accuracy of the elliptical fit. Based on these findings, the $R^2$ value is expected to decrease further for hair types, such as Caucasian and African, which exhibit greater curliness and waviness than Japanese hair.

To extend the applicability of the proposed method beyond the Japanese female cohort and better accommodate complex or multimodal orientation patterns, it is necessary to validate its performance on a broader range of hair types and pursue further methodological improvements.

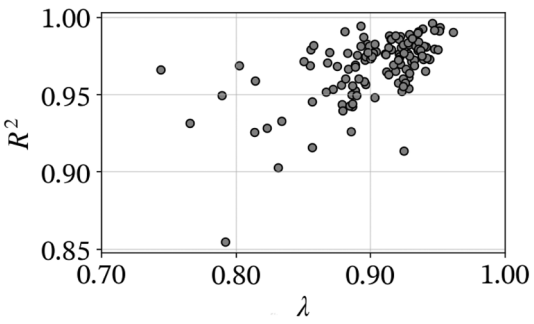


**FIGURE 4** Distribution of anisotropy index $\lambda$ and coefficient of determination $R^2$ derived from the elliptical approximation of orientation distributions across the entire data set.

## Scale robustness

We evaluated the scale robustness of the proposed method by analysing the orientation features from the data set images at varying resolutions and $f_{min}$ values. Tables 1 and 2 present the results for the orientation angle $\phi$ and the anisotropy index $\lambda$, respectively, at scales of 1/2, 1/4 and 1/8, with $f_{min} = 0.02, 0.04, 0.08$ and 0.16.

At the 1/2 scale, the mean differences in orientation angle ($\Delta\phi$) relative to the original resolution were nearly 0.3°, and the standard deviations ranged from 0.3° to 0.5° across all $f_{min}$ values. Mean differences in the anisotropy index ($\Delta\lambda$) were also negligible. These results indicate that the orientation features remained largely unchanged at this scale, demonstrating robustness.

However, at scales of 1/4 and 1/8, both the mean and standard deviation of $\Delta\phi$ increased, indicating growing bias and uncertainty in orientation angle estimation. Simultaneously, the mean of $\Delta\lambda$ became increasingly negative, which suggested a systematic underestimation of anisotropy. The corresponding rise in the standard deviation of $\Delta\lambda$ also reflects decreased reliability in the measurement at lower resolutions.

Regarding the effect of $f_{min}$, the results show that changes in this parameter had a relatively minor impact on $\Delta\phi$ across all scales. At each scale level, the mean differences remained stable, regardless of $f_{min}$, and the standard deviations showed only a slight variation. This suggests that the estimation of the principal orientation angle was relatively robust to the choice of $f_{min}$.

In contrast, $\Delta\lambda$ exhibited greater sensitivity to $f_{min}$. At lower scales, particularly at 1/8, increasing $f_{min}$ reduced the magnitude of the negative bias in $\Delta\lambda$ and slightly decreased its standard deviation. This trend indicates that higher $f_{min}$ values help preserve anisotropic features by filtering out low-frequency components that may obscure the directional structure. Therefore, although the orientation angle estimation is stable across $f_{min}$ values, a higher $f_{min}$ setting is beneficial for the anisotropy estimation, particularly at lower image resolutions.

The individual examples shown in Figure 5 provide further insight into the effects of scale variation. Figure 5a displays the original image and the corresponding analysis. At a high resolution of 0.1 mm/pixel,

**TABLE 1** Differences in the principal orientation angle $\Delta\phi$ (degrees) between the original-scale image and scaled images.

| Scale | $f_{min} = 0.02$ | $f_{min} = 0.04$ | $f_{min} = 0.08$ | $f_{min} = 0.16$ |
|---|---|---|---|---|
| 1/2 | 0.1 ± 0.4 | 0.1 ± 0.3 | 0.1 ± 0.3 | 0.2 ± 0.5 |
| 1/4 | 0.3 ± 0.9 | 0.3 ± 1.0 | 0.3 ± 1.0 | 0.5 ± 1.4 |
| 1/8 | 0.6 ± 2.1 | 0.7 ± 2.0 | 0.6 ± 2.1 | 0.6 ± 2.6 |

*Note*: Values are presented as mean ± standard deviation.

| Scale | $f_{min} = 0.02$ | $f_{min} = 0.04$ | $f_{min} = 0.08$ | $f_{min} = 0.16$ |
|---|---|---|---|---|
| 1/2 | $-0.00 \pm 0.00$ | $-0.00 \pm 0.01$ | $-0.00 \pm 0.01$ | $-0.00 \pm 0.02$ |
| 1/4 | $-0.05 \pm 0.02$ | $-0.04 \pm 0.02$ | $-0.04 \pm 0.02$ | $-0.04 \pm 0.03$ |
| 1/8 | $-0.20 \pm 0.08$ | $-0.17 \pm 0.06$ | $-0.15 \pm 0.06$ | $-0.14 \pm 0.08$ |

*Note*: Values are presented as mean ± standard deviation.

**TABLE 2** Differences in the anisotropy index $\Delta\lambda$ between the original-scale image and scaled images.

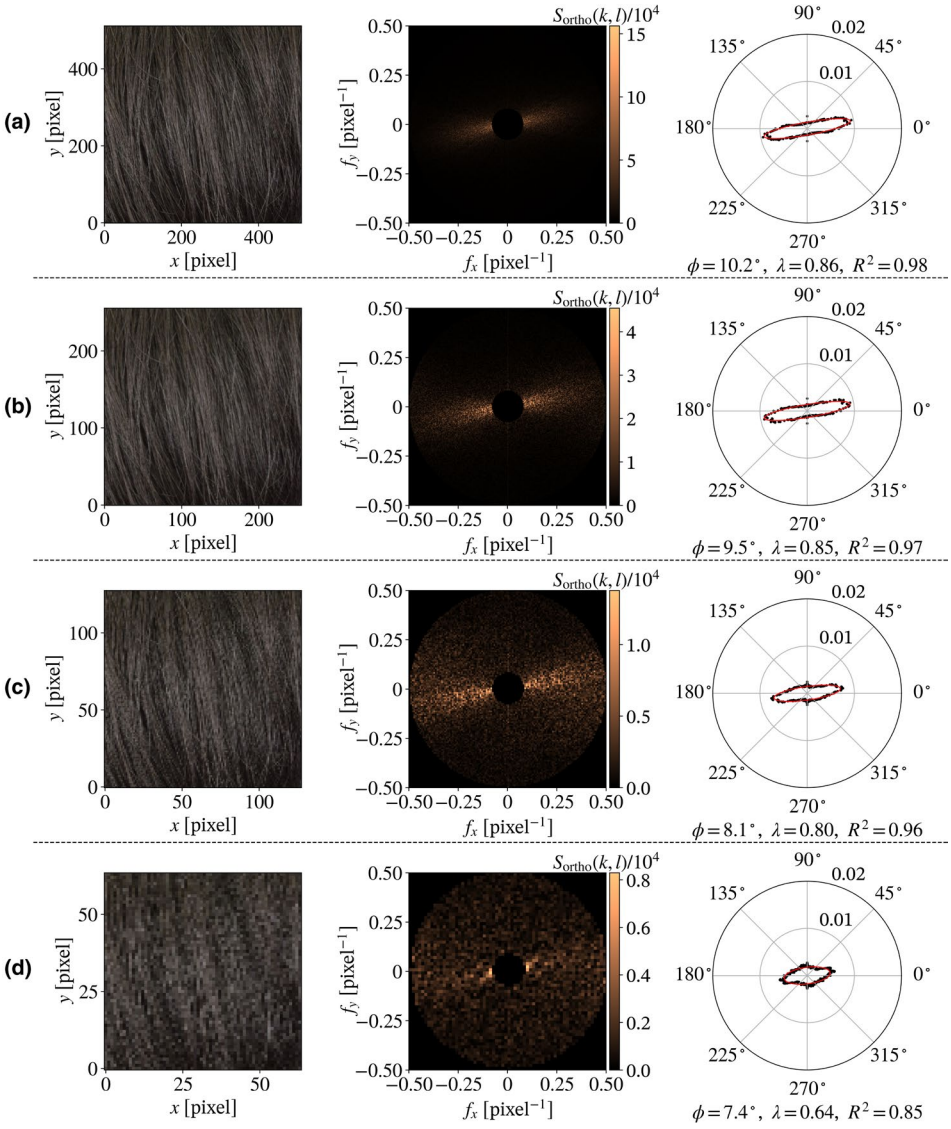


**FIGURE 5** Representative results of fibre orientation analysis for (a) the original image and the downsampled images at (b) 1/2, (c) 1/4 and (d) 1/8 of the original resolution. Each row shows, from left to right: The hair image, its corresponding Fourier spectrum $S_{ortho}(k, l)$ and the orientation distribution $P(\theta)$ (black dots) overlaid with the fitted elliptical model $\widetilde{P}(\theta)$ (red line). In the Fourier spectra, black regions indicate low-frequency components excluded from the summation in Equation (5).

individual hair fibres are resolved, allowing for accurate extraction of orientation features. Figure 5b shows an image at half scale (0.2 mm/pixel), where hair fibres remain visible and the orientation distribution closely resembles that of the original. In contrast, Figure 5c (1/4 scale, 0.4 mm/pixel) reveals a loss of clarity in individual fibres, resulting in a broader orientation distribution and underestimation of both $\phi$ and $\lambda$. At the 1/8 scale (0.8 mm/pixel), shown in Figure 5d, individual fibres are no longer discernible, resulting in an inaccurate estimation of orientation features.

These findings suggest that the clear visibility of individual hair fibres is essential for reliable orientation analysis. Within the range in which the fibres remain discernible, the proposed method demonstrates robustness to scale variations.

## General discussion

Building on these results, this section explores the broader significance, limitations and future directions of the proposed method. We present a streamlined and robust approach for quantifying hair fibre orientation using the 2D-DFT, enabling the extraction of two key directional features: the principal orientation angle ($\phi$) and anisotropy index ($\lambda$). The primary advantage of this method lies in its computational simplicity and robustness to the image scale, allowing its application to standard digital images without requiring specialized equipment. These features make it a promising tool for hair science research and for practical diagnostic applications in the beauty industry.

A key contribution of this study is the demonstration of the robustness of the scale of the method, a critical requirement for its practical deployment in real-world scenarios where the image resolution may vary. This robustness can be primarily attributed to the analysis procedure design, which is computed by aggregating the spectral amplitudes across directions. This process is inherently independent of the spatial frequency magnitude. Consequently, in principle, changes in image magnification do not affect the extracted orientation features.

However, to maintain robustness, individual hair fibres must be sufficiently resolved in the image. When the resolution drops to the point where the fibres appear blurred (e.g. Figure 5c,d), the high-frequency components that constitute the directional information are lost. This degradation in the signal quality reduces the clarity of the orientation distribution, resulting in less reliable feature extraction (Tables 1 and 2). Therefore, a practical requirement for applying this method is that the image resolution must be sufficiently high to distinguish individual fibres, and our results suggest a resolution of approximately 0.2 mm/pixel or higher.

Despite its strengths, this study has several limitations. First, the data set was limited to Japanese females, whose hair predominantly exhibited a straight or wavy texture. Validation in a more diverse population spanning a broader range of ethnicities and hair types is necessary to assess the generalizability of the method.

Second, although the method is assumed to be insensitive to hair colour owing to its reliance on structural rather than chromatic features, this assumption has not been empirically validated. In practice, grey or locally bleached hair may introduce intensity variations that could amplify the directional bias in the orientation distribution, potentially skewing the results.

A more substantial limitation arises from the fundamental assumption of a unimodal orientation distribution that underlies the use of a single elliptical model. As shown in our analysis of wavy hair (Figure 3c), this assumption breaks down for hair with complex structures, such as multiple dominant orientations. In such cases, the method fits a single ellipse to a multimodal distribution, resulting in a principal orientation angle ($\phi$) that reflects an ambiguous average, and an anisotropy index ($\lambda$) that fails to distinguish between random noise and structured, multi-directional patterns. This ambiguity limits the interpretability of the extracted features. Consequently, the current global approach cannot fully capture the structural complexity of textured hair, which reduces its effectiveness for wavy, curly and intricately styled hair.

These limitations suggest several directions for future research. A key priority is to validate the method using a broader range of hair types and ethnic groups to confirm its general applicability. To address the challenge of analysing complex hairstyles, incorporating a local analysis framework, such as the sliding window approach, is a critical next step. This enables the detection of spatially varying orientation patterns, providing a more detailed and nuanced representation of the hair structure than that achievable with a single global estimate.

In addition to extending its applicability, the core methodology offers opportunities for refinement. A promising direction involves the role of the exponent $q$ in computing the Fourier spectrum. While this study used $q = 1$ to reflect the amplitude, alternative settings, such as $q = 2$ (power) [18] or other real-valued exponents, may emphasize different structural components. A systematic exploration of $q$ would allow researchers to tune the sensitivity of the method to either dominant or subtle directional features. This line of investigation could result in a more flexible and generalized framework for analysing the rich diversity of hair textures, and thus represents a compelling direction for future research.

## CONCLUSION

In this study, we proposed a simple and robust method for quantifying hair orientation based on the 2D-DFT. The technique enables direct extraction of the principal orientation angle ($\phi$) and the anisotropy index ($\lambda$) from standard digital images, without requiring specialized equipment. This method is also robust to changes in image scale, which is an essential requirement for practical deployment across diverse imaging environments.

Although further validation of a broader variety of hair types and the integration of local analysis to handle multiple orientation components are required, the proposed method overcomes the major limitations of existing techniques in terms of accessibility and broad applicability. Overall, this approach provides a solid foundation for objective hair appearance analysis, with strong potential for

applications in both hair science research and as diagnostic tools within the beauty industry.

## ACKNOWLEDGEMENTS

The authors have nothing to report.

## CONFLICT OF INTEREST STATEMENT

The authors declare no competing interests.

## DATA AVAILABILITY STATEMENT

The data set analysed in the current study is not publicly available because of restrictions imposed by the ethics committee to protect participant confidentiality. Requests for access to data will be reviewed on a case-by-case basis, subject to institutional review board approval and must align with the originally approved terms of use.

## ETHICS STATEMENT

Ethical approval for this study was granted by the Brain Care Clinic Institutional Review Board under study protocol number 20171211 and management number BCC241003-5.

## ORCID

*Motoki Takeda* https://orcid.org/0009-0007-1822-0692

## REFERENCES

1. Cash TF. The psychology of hair loss and its implications for patient care. Clin Dermatol. 2001;19(2):161–6. https://doi.org/10.1016/S0738-081X(00)00127-9
2. Manning J. The sociology of hair: hair symbolism among college students. Soc Sci J. 2010;10:11.
3. Ellis-Hervey N, Doss A, Davis D, Nicks R, Araiza P. African American personal presentation: psychology of hair and self-perception. J Black Stud. 2016;47(8):869–82. https://doi.org/10.1177/0021934716653350
4. Kamikado J, Toyota Y, Fujiwara N, Kobayashi K, Suzuta K, Joko K. Mechanism of frizz phenomenon occurring in bleached hair. J Soc Cosmet Chem Japan. 2023;57(3):251–64. https://doi.org/10.5107/sccj.57.251
5. Sinclair RD. Healthy hair: what is it? J Investig Dermatol Symp Proc. 2007;12(2):2–5. https://doi.org/10.1038/sj.jidsymp.5650046
6. Cruz CF, Costa C, Gomes AC, Matamá T, Cavaco-Paulo A. Human hair and the impact of cosmetic procedures: a review on cleansing and shape-modulating cosmetics. Cosmetics. 2016;3(3):26. https://doi.org/10.3390/COSMETICS3030026
7. Fernandez-Flores A, Saeb-Lima M, Cassarino DS. Histopathology of aging of the hair follicle. J Cutan Pathol. 2019;46(7):508–19. https://doi.org/10.1111/cup.13467
8. Tajima M, Hamada C, Arai T, Miyazawa M, Shibata R, Ishino A. Characteristic features of Japanese women's hair with aging and with progressing hair loss. J Dermatol Sci. 2007;45(2):93–103. https://doi.org/10.1016/J.JDERMSCI.2006.10.011
9. Hrdy D. Quantitative hair form variation in seven populations. Am J Phys Anthropol. 1973;39(1):7–17. https://doi.org/10.1002/ajpa.1330390103
10. Loussouarn G, Garcel AL, Lozano I, Collaudin C, Porter C, Panhard S, et al. Worldwide diversity of hair curliness: a new method of assessment. Int J Dermatol. 2007;46(Suppl. 1):2–6. https://doi.org/10.1111/j.1365-4632.2007.03453.x
11. Robbins CR. Chemical and physical behavior of human hair. Berlin, Heidelberg: Springer Berlin Heidelberg; 2012. https://doi.org/10.1007/978-3-642-25611-0
12. Lechocinski N, Breugnot S. Fiber orientation measurement using polarization imaging. J Cosmet Sci. 2011;62(2):85–100.
13. Dalal N, Triggs B. Histograms of oriented gradients for human detection. In: 2005 IEEE Computer Society Conference on Computer Vision and Pattern Recognition (CVPR'05). 2005. p. 886–93. https://doi.org/10.1109/CVPR.2005.177
14. Daniels G, Tamburic S, Benini S, Randall J, Sanderson T, Savardi M. Artificial intelligence in hair research: a proof-of-concept study on evaluating hair assembly features. Int J Cosmet Sci. 2021;43(4):405–18. https://doi.org/10.1111/ICS.12706
15. McMullen RL, Zhang G, Gillece T. Quantifying hair shape and hair damage induced during reshaping of hair. J Cosmet Sci. 2015;66(6):379–409.
16. Pourdeyhimi B, Dent R, Davis H. Measuring fiber orientation in nonwovens part III: Fourier transform. Text Res J. 1997;67(2):143–51. https://doi.org/10.1177/004051759706700211
17. Ayres CE, Jha BS, Meredith H, Bowman JR, Bowlin GL, Henderson SC, et al. Measuring fiber alignment in electrospun scaffolds: a user's guide to the 2D fast Fourier transform approach. J Biomater Sci Polym Ed. 2008;19(5):603–21. https://doi.org/10.1163/156856208784089643
18. Enomae T, Han Y-H, Isogai A. Nondestructive determination of fiber orientation distribution of paper surface by image analysis. Nord Pulp Paper Res J. 2006;21(2):253–9. https://doi.org/10.3183/npprj-2006-21-02-p253-259
19. Lowe DG. Distinctive image features from scale-invariant keypoints. Int J Comput Vis. 2004;60(2):91–110. https://doi.org/10.1023/B:VISI.0000029664.99615.94
20. Loussouarn G, Lozano I, Panhard S, Collaudin C, el Rawadi C, Genain G. Diversity in human hair growth, diameter, colour and shape. An in vivo study on young adults from 24 different ethnic groups observed in the five continents. Eur J Dermatol. 2016;26(2):144–54. https://doi.org/10.1684/EJD.2015.2726
21. Bradski G. The OpenCV library. Dr Dobb's Journal of Software Tools. 2000.

**How to cite this article:** Takeda M, Lee S, Kiyono K. Scale-robust fibre orientation analysis of hair using two-dimensional Fourier transform. Int J Cosmet Sci. 2025;00:1–10. https://doi.org/10.1111/ics.70052